Impurity Control in Improved H-mode Scenarios in ASDEX Upgrade

C.F. Maggi, R. Dux, L.D. Horton, R. Neu, D. Nishijima, T. Pütterich, A.C.C. Sips,

B. Zaniol[1] and ASDEX Upgrade Team

MPI für Plasmaphysik, EURATOM Association, D-85748 Garching, Germany

[1]Consorzio RFX, EURATOM Association, Padova, Italy

1. Introduction

ASDEX Upgrade (AUG) is playing a leading role in the development of scenarios in which the confinement and stability of a standard H-mode are improved. The main features of this regime, low central shear and absence of sawteeth activity, are obtained by early heating of the discharge using a combination of on- and off-axis neutral beams (NB) [1]. The operation space of the improved H-mode on AUG has been extended significantly in 2004 in terms of q_{95}, ρ^*, as well as testing combined NB and RF heating and the use of ECCD.

The present work addresses the behaviour and control of core impurities in this regime, in AUG, with a mix of plasma facing components (PFC's) of carbon and tungsten, allowing the study of low and high-Z intrinsic impurities in the same tokamak.

In the 2004 campaign, about 65% of the area of PFC's is coated with W [2, 3]. A major concern in improved H-modes, which are characterized by substantially peaked electron density profiles compared to standard H-modes, is impurity accumulation, especially for high-Z impurities. Accumulation of W inside $\rho < 0.3$ in NB heated improved H-modes has indeed been reported [4]. However, the application of central ECRH, increasing strongly the anomalous diffusion and flattening the plasma density profile, led to a suppression of high-Z impurity accumulation. The injection of central ICRH is also commonly employed to reduce density peaking [5].

In this work the low-Z impurity densities (C and Ne) are obtained from CXRS using a machine independent CX analysis package [6] linked with ADAS. The core W concentrations are extracted from the central line emission of W^{46+} (SXR) [7].

2. Improved H-mode scenarios at AUG

A figure of merit for fusion gain is $H_{98} \cdot \beta_N / q_{95}^2$, where H_{98} is the H factor (ITER98 (y,2) scaling), β_N is the normalized beta and q_{95} the safety factor at the 95% flux surface. In the past, the bulk of improved H-modes in AUG was obtained at $q_{95} \sim 4$, because of easier access to the regime. Experiments in 2004 have extended the operation domain in four different areas: (1) operation over a range of q_{95} from 3.2 to 4.4 (at Ip = 1MA) at $\beta_N \sim 2.7$-3.0 with NB heating only (series labelled 'q scan' in the following).

(2) Since in a reactor control of the current profile in the current ramp-up phase may be difficult, improved H-modes were obtained starting from a standard H-mode discharge with on-axis NB heating only and adding central counter ECCD to suppress the sawteeth [8] (series labelled 'NBI+ECCD'). These discharges (Ip = 1MA /Bt = 2.4T, q_{95}

= 4.5) were run at the high end of the explored q_{95} range to enable central ECCD. At present the length of the ECRH phase in AUG is limited to 2s.

(3) In standard H-modes at $q_{95} \sim 3$ NTM's are seeded by sawteeth and their onset scales unfavourably with $\rho*$. A dedicated experiment was therefore performed to measure the $\rho*$ dependence of the maximum stable β_N in improved H-modes, where the NTM trigger is absent. The widest possible range of $\rho*$ on AUG, at fixed $q_{95} \sim 4$, implied a variation from Ip = 0.6 MA / Bt = 1.4 T to Ip = 1.2 MA / Bt = 2.8 T, resulting in $\rho*_D$ = $12.2 \cdot 10^{-3} - 8.6 \cdot 10^{-3}$ (series labelled '$\rho*$ scan'). The maximum β_N obtained (~ 3) was found to be independent of $\rho*$.

(4) Improved H-modes were also achieved with RF powers up to $P_{ICRH} \sim P_{NBI}$ with β_N ~ 2.3-2.4 at the maximum available ICRH power (5 MW nominal launched) at $q_{95} \sim 3.7$. The value of β_{pol} was maintained by feedback control on the NB power. No sawteeth were observed in these scenarios, only small amplitude NTM's, which however did not limit the maximum β_N.

In this series of discharges (labelled 'NBI+ICRH') trace Ne was puffed to investigate the transient transport properties of low-Z impurities using CXRS.

3. Impurity behaviour in AUG improved H-modes

The analysis shows that in improved H-mode discharges the electron density profiles are typically peaked, with peaking factors ranging from 1.6 to ~ 2, defined here as the ratio of the density at $\rho = 0.1$ (plasma core) and at $\rho = 0.9$ (pedestal region). In general, improved H-modes with highly peaked density profiles are characterized by high core C and W concentrations, $c_C \sim 2$-3% and $c_W \geq 10^{-4}$, while for lower peaking factors $c_C \sim 1$-2% and $c_W \sim 10^{-5}$, as shown in Fig. 1.

In the q-scan series, both at low and high q_{95}, the core c_C reached values of $\sim 2.5\%$ and the core c_W was high, $\geq 10^{-4}$. Optimization of the discharge with the addition of central ICRH heating is needed to reduce the core impurity content.

In the NBI+ECCD series, during the phase with ECCD, the C density profiles were flat and the core c_C remained constant to $\sim 1\%$, but rose continuously to 3% or more till the end of the pulse after the ECCD was switched off. Consistent with previous findings, W accumulation in the core was suppressed during the ECCD phase, while c_W immediately rose to values $\geq 10^{-4}$ as soon as the ECCD was switched off. Density peaking factors of 1.6-1.8 are found in the phase with ECCD, while they reach values of 2.0-2.2 after the ECCD is switched off. Similar results were found with central co-ECCD, when (small) sawteeth were present, as expected [10]. Injecting the same amount of central ECRH power, but without CD, into a reference improved H-mode was less efficient in reducing c_W, whereas c_C did not rise above 1.5% in the core (labelled 'NBI+ECRH').

In the $\rho*$ scan, at low Ip the C density profiles are flat and $c_C \sim 1\%$. This is presumably related to a larger fraction of NB heating reaching the core due to the lower

density in these discharges (a point for future quantitative analysis of these experiments with transport codes). c_W in the core remains at values $\sim 10^{-5}$ or cannot be deduced since the low T_e shifts the W ionization balance from W^{46+} to lower ionization stages. At high Ip, a first attempt at the discharge with only 1.4 MW of ICRH leads to a peaking factor of ~ 1.9, a steady increase of c_C up to 3% and $c_W \geq 10^{-4}$. By increasing P_{ICRH} to 3MW, the density peaking is reduced to ~ 1.6, core W accumulation is suppressed and c_C is $\leq 1\%$.

With a substantial fraction of RF power, the NBI+ICRH discharges have a moderate density peaking factor (~ 1.5) and flat C and Ne density profiles, with $c_C \sim 1\%$ in the core. The core c_W remains low to $\sim 10^{-5}$. When the injected ICRH power is dropped from 5MW (#19088,19089) to 3MW (#19090) at $P_{heat} \sim 8MW$ and later in the pulse at $P_{heat} \sim 10MW$, the density peaking increases up to 2.0 and c_W reaches values $\geq 10^{-4}$. The Ne density profiles become significantly peaked in the later phase of the discharge. Although the C density could not be measured in this discharge, the similarity in shape of the C and Ne density profiles for pulses #19088 and #19089 point to C accumulation as well in #19090.

The diffusion D and convective v/D transport coefficients for Ne are derived [9] from the measured Ne density profiles of discharges #19089 and #19090 (Fig. 2). The effect of the reduction of central ICRH heating from #19089 to #19090 can be distinguished by the lower diffusivity and higher inward pinch for Ne impurities in #19090. The maximum time resolution of the CXRS diagnostic (10 ms) is adequate also for the derivation of D inside $\rho_{pol} \leq 0.6$.

4. Impurity control and compatibility with improved H-mode performance

Because of the moderate plasma densities ($\sim 5\text{-}8 \cdot 10^{19}$ m^{-3}) typical of this regime, high impurity concentrations, c_C up to 2-3% and $c_W \sim 10^{-4}$, are compatible with improved H-mode operation and performance in AUG (Fig. 3, top). Future analysis will however have to address how these values extrapolate to ITER, where c_W must be kept well below 10^{-4} to allow for a sizeable operational window in the presence of other impurities [10].

Future optimisation of the improved H-mode scenario in AUG will require integration of the improved performance connected with density peaking with control of impurity accumulation along the path already started in 2004 (Fig. 3, bottom). This integration will be facilitated by the new, long pulse ECCD system, presently being installed on AUG.

References:

[1] A.C.C. Sips et al., Plasma Phys. Control. Fusion **44** (2002) B69.

[2] R. Neu et al., this conference.

[3] R. Dux et al., PSI 2004, submitted to J. Nucl. Mater.

[4] R. Dux et al., Plasma Phys. Control. Fusion **45** (2003) 1815.

[5] J. Stober et al., Nucl. Fusion **43** (2003) 1265.

[6] C.F. Maggi et al., Proc. 30th EPS Conf. on Control. Fusion and Plasma Phys., 2003, Vol. 27A, P-1.63.

[7] R. Neu et al., IPP report 10/25, 2003.

[8] A. Mück et al., Proc. 30th EPS Conf. on Control. Fusion and Plasma Phys., 2003, Vol. 27A, P-1.131.

[9] R. Dux et al., Nucl. Fusion **39** (1999) 1509.

[10] R. Neu et al., Fusion Engineering and Design **65** (2003) 367.
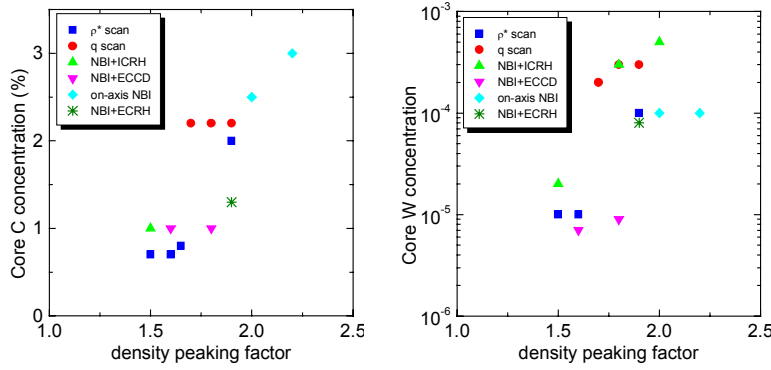
Figure 1. Core C and W concentrations versus electron density peaking factor.
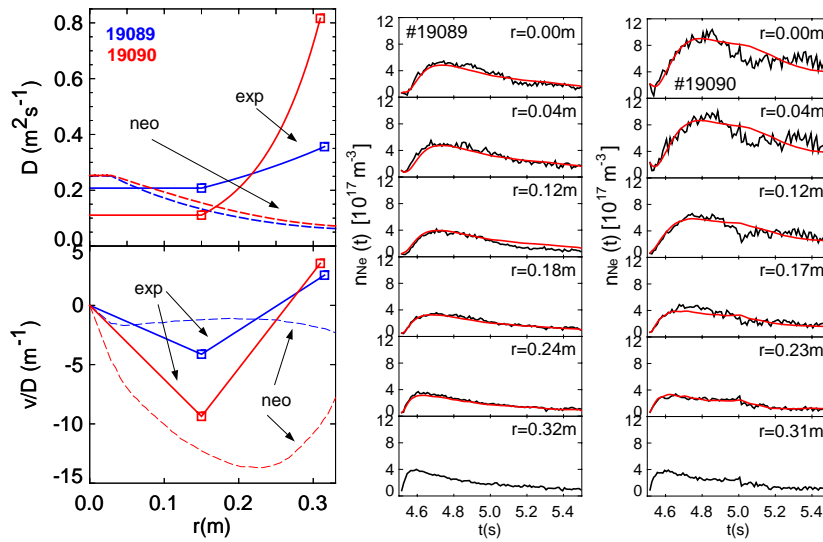
Figure 2. **Left:** D and v/D coefficients for Ne for varying ratios of P_{ICRH}:P_{NBI} (5:5) #19089, (3:5) #19090: experiment and comparison with neoclassical theory. The Ne puff was at 4.5 s. **Right:** Time evolution of the Ne density profiles from CXRS and χ^2 fit, from which the transport coefficients are derived. The density at r = 0.32 (ρ_{pol} ~ 0.6) is used as boundary condition.
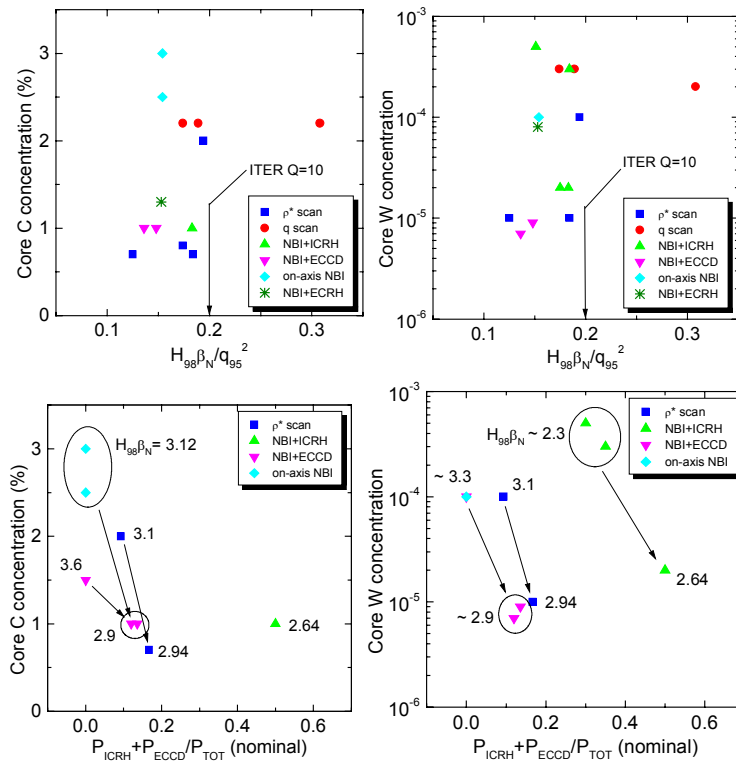
Figure 3. Top: core C and W concentrations vs figure of merit for fusion gain. **Bottom:** control of light and heavy impurity content in the core of AUG improved H-modes using central ICRH or ECCD. In the 'NBI+ICRH' discharges at lower P_{ICRH} the C density measurements were replaced by those of Ne, following Ne gas puffing.